JOURNAL OF GEOPHYSICAL RESEARCH: OCEANS, VOL. 118, 3670–3678, doi:10.1002/jgrc.20268, 2013

Northern North Atlantic sea surface height and ocean heat content variability

Sirpa Häkkinen,[1] Peter B. Rhines,[2] and Denise L. Worthen[3]

Received 8 March 2013; revised 7 June 2013; accepted 7 June 2013; published 30 July 2013.

[1] The evolution of nearly 20 years of altimetric sea surface height (SSH) is investigated to understand its association with decadal to multidecadal variability of the North Atlantic heat content. Altimetric SSH is dominated by an increase of about 14 cm in the Labrador and Irminger seas from 1993 to 2011, while the opposite has occurred over the Gulf Stream region over the same time period. During the altimeter period the observed 0–700 m ocean heat content (OHC) in the subpolar gyre mirrors the increased SSH by its dominantly positive trend. Over a longer period, 1955–2011, fluctuations in the subpolar OHC reflect Atlantic multidecadal variability (AMV) and can be attributed to advection driven by the wind stress "gyre mode" bringing more subtropical waters into the subpolar gyre. The extended subpolar warming evident in SSH and OHC during the altimeter period represents transition of the AMV from cold to warm phase. In addition to the dominant trend, the first empirical orthogonal function SSH time series shows an abrupt change 2009–2010 reaching a new minimum in 2010. The change coincides with the change in the meridional overturning circulation at 26.5°N as observed by the RAPID (Rapid Climate Change) project, and with extreme behavior of the wind stress gyre mode and of atmospheric blocking. While the general relationship between northern warming and Atlantic meridional overturning circulation (AMOC) volume transport remains undetermined, the meridional heat and salt transport carried by AMOC's arteries are rich with decade-to-century timescale variability.

Citation: Häkkinen, S., P. B. Rhines, and D. L. Worthen (2013), Northern North Atlantic sea surface height and ocean heat content variability, *J. Geophys. Res. Oceans*, *118*, 3670–3678, doi:10.1002/jgrc.20268.

1. Introduction

[2] Global analysis of ocean surface height (SSH) variability and water column heat content (OHC) is increasingly important: both global warming, which is dominantly stored as OHC, and unforced variability of circulation are involved. SSH variability is more readily observed, and its strong, yet regionally dependent, covariability with OHC is important to diagnose: global patterns, for example, displayed by *Willis et al*. [2004], are complex in both space and time. While there is significant thermosteric correlation of SSH and OHC variability, regional circulation dynamics are important in the North Atlantic such as climatic episodes of warm, saline northern Atlantic Ocean occurring at decadal to century timescales. These events covary with a weak subpolar gyre and increased advection of a deep-reaching branch of warm subtropical waters to the subpolar gyre [*Häkkinen et al*., 2011a]. These intrusions appear to coincide with the relaxation of both gyres in response to the weak phase of the wind stress curl "gyre mode." In the weak phase of the gyre mode the isopycnal tilt decreases in both gyres, so that the subpolar gyre contracts but the subtropical gyre expands which allows the increased escape of subtropical waters to the subpolar gyre. This mechanism is supported by observations and by numerical model studies which show the westward movement of the polar front in the weak gyre mode of the late 1990s [*Desbruyeres et al*., 2013; *Sarafanov et al*., 2008; *Bersch et al*., 2007; *Hátún et al*., 2005].

[3] The concept of a gyre mode was introduced by *Hátún et al*. [2005] based on the time series of the first SSH empirical orthogonal function (EOF) mode. We expanded its definition to be synonymous with the time series of the second wind stress curl EOF mode [*Häkkinen et al*., 2011a]. (The first EOF of wind stress curl resembles the curl associated with the North Atlantic Oscillation, while its principal component (PC) time series is similar to NAO, the spatial pattern of North Atlantic Oscillation (NAO) is different, as described later.) The wind stress curl gyre mode has a simple relationship with the average sea level pressure (SLP) over the subpolar gyre, such that the weak

Additional supporting information may be found in the online version of this article.

[1]NASA Goddard Space Flight Center, Greenbelt, Maryland, USA.
[2]School of Oceanography, University of Washington, Seattle, Washington, USA.
[3]Wyle ITS and NASA Goddard Space Flight Center, Greenbelt, Maryland, USA.

Corresponding author: S. Häkkinen, NASA Goddard Space Flight Center, Code 615, Greenbelt, MD 20771, USA. (sirpa.hakkinen@nasa.gov)

2169-9275/13/10.1002/jgrc.20268

gyre has a positive SLP anomaly. This SLP pattern could be interpreted as the Eastern Atlantic pattern (EAP) which is shown by *Scherrer et al*. [2006] to have a linkage to atmospheric blocking. As a consequence, the gyre mode can be associated with fluctuations in the storm track position as a result of atmospheric blocking activity. Blocking activity, essentially related to large meanders of the jet stream that persist typically for 4–8 days and can occur in clusters during a winter season, appears to have multidecadal fluctuations, which covary with the Atlantic multidecadal oscillation/variability (AMO/AMV) [*Häkkinen et al*., 2011b, hereinafter referred to as HRW]. AMO is defined as an area weighted average sea surface temperature for the region 0°–60°N, 80°W–10°E from which either a linear trend or a forced signal, "the global warming signal," is removed [*Ting et al*., 2009]. AMO/AMV typically has an out-of-phase variability in the South Atlantic. It has been linked into numerous climate processes in the surrounding continents, e.g., rainfall and droughts in NE Brazil and in Sahel, and Atlantic hurricanes [*Enfield et al*., 2001; *McCabe et al*., 2004; *Knight et al*., 2006]. AMO/AMV has been also linked to the Atlantic meridional overturning circulation (AMOC) [e.g., *Knight et al*., 2005].

[4] Our earlier work on the altimetric SSH data shows a steady increase of the subpolar SSH which we interpreted as a decline of the circulation strength in the subpolar gyre from 1992 to 2003 [*Häkkinen and Rhines*, 2004]. The associated changes in geostrophic currents are clearly visible in altimetric images of the subpolar boundary current in Labrador and Irminger seas. However, the high eddy activity and fluctuations of the Gulf Stream-North Atlantic Current (GS-NAC) system core camouflage any changes in the strength of the eastern region of the subtropical gyre. Now with almost 20 years of altimeter data we will present an update to this record in section 3. In section 4 we will discuss the changes in the observed ocean heat content (OHC) which are shown to concentrate along the subpolar boundary currents in support of our view of the gyre mode effects on the subpolar circulation. Finally, in section 5 we discuss changes in the SSH time series and their relation to atmospheric blocking.

2. Data

[5] Altimetry data for the sea surface height was acquired from the NASA MEaSUREs (Making Earth System Data Records for Use in Research Environments) database with 1° × 1° resolution (October 1992 to May 2012) as well as from AVISO (Archiving, Validation, and Interpretation of Satellite Oceanographic data), a multisatellite product at 1/3° resolution (October 1992 to December 2011) to distinguish changes in the boundary currents. Ocean heat content (OHC) data for the 0 to 700 m water column and pentadal hydrographic data (1955–2011) were acquired from the NOAA/NODC database. The atmospheric data from National Center for Environmental Prediction/National Center for Atmospheric Research (NCEP/NCAR) Reanalysis is used to derive the wind stress curl for the EOF analysis and to compute the winter blocking index for the subpolar region as in HRW. In Table 1 we show December-March blocking days for area 45°N–75°N, 70°W–10°E, and also subdivided by longitude 30°W into a western box, Greenland blocking, and an eastern box, the western European blocking. During the altimeter era the most active wintertime Greenland blocking (50 or more days out of 120) has occurred in winters 1996, 2001, 2005, 2010, and 2011, while the winters 1993, 1996, 2005, 2006, 2007, and 2012 had the most active western European blocking with 75 or more blocking days. Table 1 also shows the station-based NAO index from http://www.cgd.ucar.edu/cas/jhurrell/indices.html. The increased Greenland blocking is associated with negative NAO [*Woollings et al*., 2008], while western European blocks occur during both phases of the NAO index.

Table 1. Winter Blocking Days and NAO for 1990–2012[a]

Year	SPG West	SPG East	All SPG	NAO
1990	28	48	54	3.96
1991	16	51	51	1.03
1992	16	80	81	3.28
1993	7	80	80	2.67
1994	14	51	52	3.03
1995	11	20	20	3.96
1996	50	95	103	−3.78
1997	30	67	71	−0.17
1998	23	47	59	0.72
1999	12	43	46	1.70
2000	17	65	67	2.80
2001	52	64	83	−1.90
2002	36	56	63	0.76
2003	20	73	77	0.20
2004	36	49	56	−0.07
2005	66	80	94	0.12
2006	28	76	83	−1.09
2007	42	81	82	2.79
2008	5	28	33	2.10
2009	27	58	66	−0.41
2010	61	61	75	−4.64
2011	52	71	94	−1.57
2012	5	78	78	3.17

[a]December-March blocking days for the whole area 45°N–75°N, 70°W–10°E (the fourth column) and also subdivided by longitude 30°W into a western box (the second column), i.e., Greenland blocking, and an eastern box, the western European blocking (the third column). Number of days for the whole area can be less than the sum of the subregions because there can be a block that extends over both subregions. For reference, the station-based NAO index (for Dec-Jan-Feb-Mar (DJFM)) is given in the fifth column from http://www.cgd.ucar.edu/cas/jhurrell/indices.html. SPG, subpolar gyre.

3. Altimetric SSH and Surface Circulation

[6] A Hovmoeller plot of SSH from October 1992 to May 2012 (from 1° × 1° MEaSUREs project; seasonal cycle removed) at longitude 45°W (Figure 1a) shows a long-term trend dominating SSH from the subpolar gyre to the tropics superimposed on strong interannual variability particularly over the Gulf Stream near its transition to the North Atlantic Current. Southward movement of a high SSH anomaly from the Gulf Stream is seen in the early 2000s, and the strong event of 2010 appears (mostly negative anomalies over the GS, positive south of 20°S and north of 45°N). The opposing trend in subpolar (SP) gyre and GS dominates the long-term behavior at 45°W displayed with 95% significance levels (Figure 1b). The

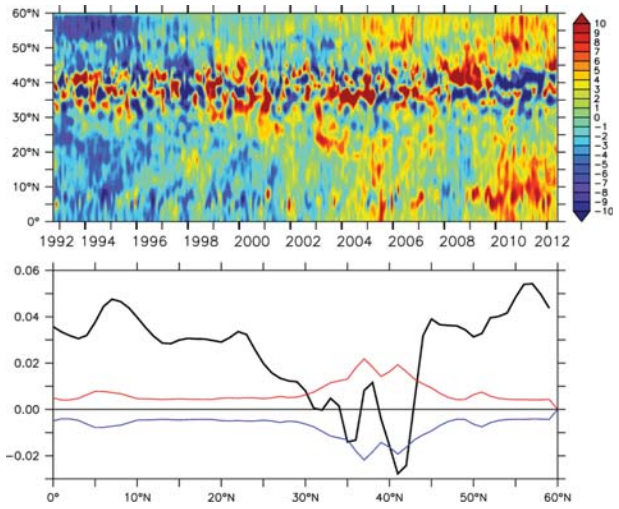

Figure 1. Hovmoeller diagram of (top) altimetric SSH anomaly from MEaSUREs project at 45°W in cm and (bottom) the trend (thick black) along the same longitude versus latitude in cm/month including the 95% significance levels (red and blue). This longitude crosses the Gulf Stream/North Atlantic Current transition region at 40°N–44°N latitude, and the activity there is associated with shifts of the bifurcating jet.

negative trend over the GS region barely reaches 95% significance due to the high eddy variability. Origin of the GS region's trend and variability can be related both to intensity of the circulation, the steric height, and heat content of the entire region encompassing the GS and its northern and southern recirculation gyres and to the latitude of the GS path [e.g., *Joyce and Zhang*, 2010; *Mahajan et al*., 2011]. However, further east a significant positive trend is present across all latitudes from the equator to 65°N suggestive of a basin-scale phenomenon such as AMO. The EOF analysis of SSH presents the spatial pattern of the basin mode with the opposing trend in the subpolar gyre and GS region (Figure 2). The pattern of the first EOF mode has not changed greatly from *Häkkinen and Rhines* [2004]; also, the time series (the principal component; PC1) shows a continued downward trend with an abrupt drop in 2010 and a minor recovery in 2011. The largest amplitude of change (SSH increase) is concentrated in the subpolar gyre.

[7] To study how the dominant boundary currents have evolved, we computed first the vector EOF for the geostrophic velocities from AVISO altimetry (Figures 3a–3c). The behavior of the vector EOF1 and PC1 for the geostrophic surface current field supports the same gyre weakening as the SSH EOF with some differences: spatial differentiation of SSH to produce velocity increases the importance of mesoscale eddies and boundary currents. PC1 now includes a strong minimum during 2005 and a recovery by 2009, however, followed by another decline. The high-resolution vector field EOF particularly singles out the boundary currents in the Irminger and Labrador seas as the foci of the changes. The North Atlantic Current (mostly omitted from the figure south of 52°N) in the Rockall Channel and Iceland Sea displays strong eddy activity which has been included partially in the EOF1, but its changes are inconclusive based on the EOF analysis. The difference between the vector fields from the late period (2007–2011; in Figure S1) and early period (1993–1997) shows weakening of the boundary current of the subpolar region. (Section 4 discusses further current and ocean heat content changes with Figures 6a and 6b.)

[8] The central Labrador Sea SSH time series is found to correlate highly with the seasonal cycle and trend of steric (baroclinic) SSH calculated from ARGO hydrographic profile data (I. Yashayaev, personal communication, 2012). The seasonal cycle amplitudes are similar for 2003–2005 yet the steric height seasonal cycle is about one-half the altimetric height cycle thereafter, suggesting a sudden barotropic change in the gyre circulation. The long-period increase of steric and altimetric height, 1992–2010, is nearly identical, suggesting dominantly baroclinic gyre deceleration. This analysis showing variability of the boundary currents is particularly important, given the difficulties sometimes found with altimetric data near coastal boundaries, and with interpreting broad SSH trends as circulation change. It also shows that within the general, long-term decline of the subpolar gyre's surface circulation, there is additional complexity; for example, the core of the Irminger Gyre actually trends stronger, while its encircling surface boundary current decelerates (as shown with intensive hydrographic surveys by *Vage et al*. [2011], using

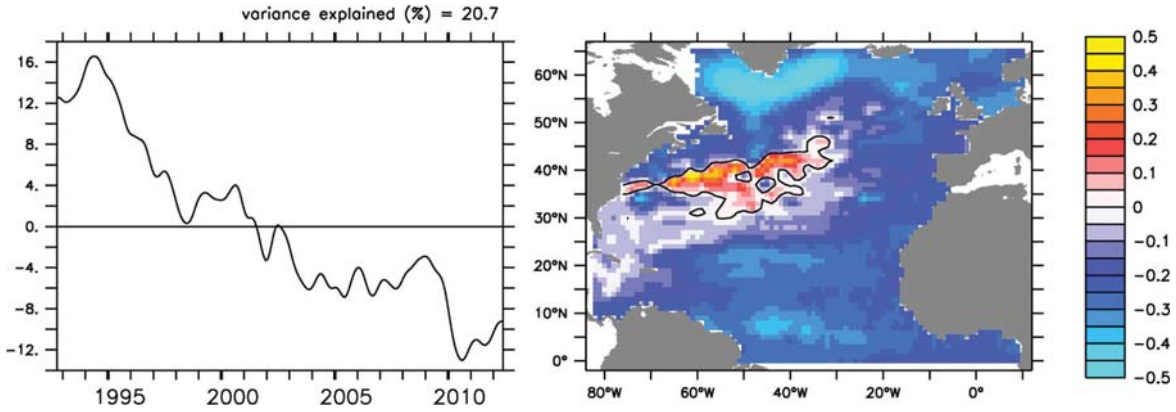

Figure 2. (left) Sea surface height PC1 in cm and (right) EOF1 (dimensionless) from 1° × 1° SSH data set from MEaSUREs project.

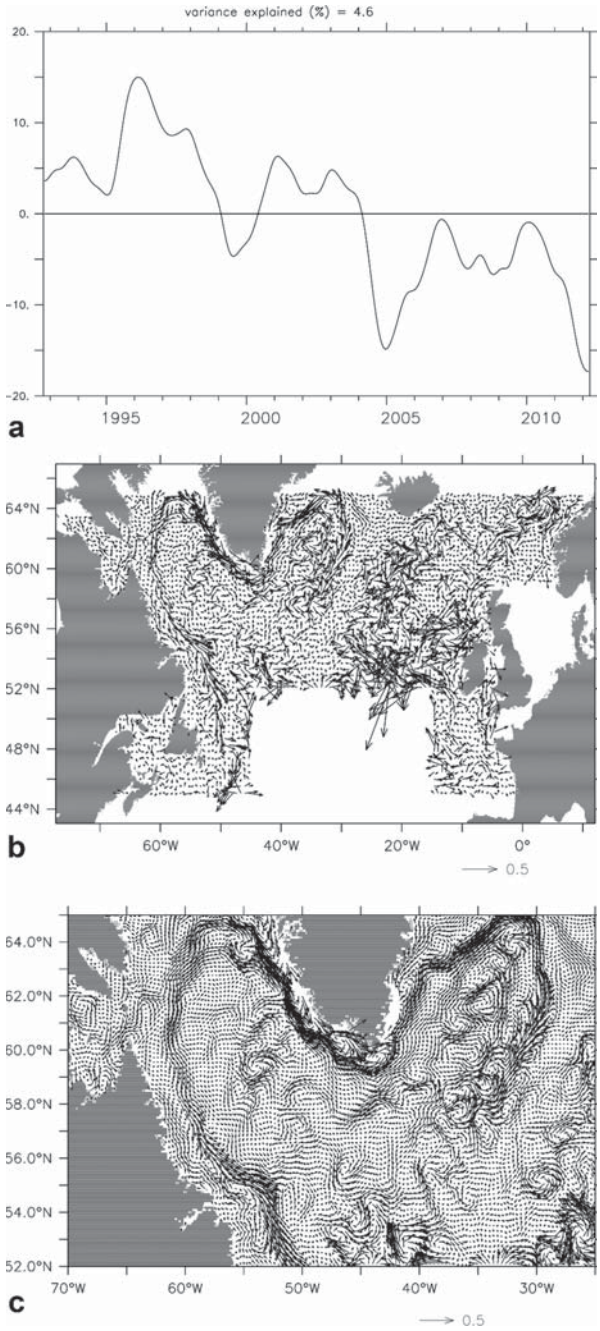

Figure 3. (a) PC1 of (b) the geostrophic vector EOF1 (only every second vector is plotted). A region over the North Atlantic current is excluded due to its high eddy variability. (c) Closer look on the EOF1 over the Irminger and Labrador seas with all vector points plotted.

repeat acoustic Doppler current profiler (adcp) sections from the transport vessel *Nuka Arctica* of *Knutsen et al*. [2005]). Complexity is also present in the vertical structure of the subpolar circulation [*Vage et al*., 2011; *Daniault et al*., 2011]. In the Irminger Basin *Vage et al*. [2011] show that the deeper Irminger circulation has accelerated, possibly related to a rebalancing of the source waters between Labrador seawater, local Irminger deep convection, and increasing inflow from the subtropics. They find the trend in SSH to be largely steric (density-related) and thus susceptible to convective forcing as well as wind stress forcing.

4. Ocean Heat Content

[9] More than 90% of the global warming of the Earth system is thought to be stored in the world ocean [*Levitus et al*., 2012]. To connect lateral heat flux and its variability over decades and longer, we address spatial structure of that warming by utilizing the NODC 0 to 700 m heat content data. We compute the subpolar area average heat content (45°N–65°N, 70°W–0°) and EOFs both for the subpolar gyre (45°N–65°N, 70°W–0°), and for the North Atlantic (0°–65°N), as well. The spatial pattern of the subpolar OHC EOF1 is dominated by anomalies of the same sign and explains 55% of all variance (Figure 4a). This same mode is the second mode of the full North Atlantic OHC (17% of variance; Figure 4b), the linear (secular) warming trend being the first mode (not shown).

[10] The full North Atlantic EOF2 pattern has strong activity over the Gulf Stream and the recirculation gyre/slope waters just north of it. This is similar to the *Zhang*'s [2008] EOF1 of temperature at 400 m depth ("Tsub") sharing a close correspondence to the altimetric SSH EOF1. Our EOF1 pattern (not shown) is dominated by the basin-average warming trend which has been removed from Zhang's data before her EOF analysis. In *Joyce and Zhang* [2010] EOF1 of Tsub is associated with the well-documented variability of the Gulf Stream's latitude. Further discussion of this pattern by *Mahajan et al*. [2011, Figure 1] (from detrended data, i.e., again, the secular warming trend has been filtered out) with updated data shows close correspondence between their SSH EOF1 and their Tsub EOF1 in an ocean model assimilation experiment.

[11] A similar pattern to OHC EOF2 is also seen by *Zhai and Sheldon* [2012] with simple difference maps for 0 to 700 m Atlantic OHC between 1955–1970 and 1980–1995. They associate these with wind stress variability, and its impact on the Sverdrup transport and lateral heat advection in the Gulf Stream/North Atlantic Current system, similar to the conclusions of *Häkkinen and Rhines* [2009] and *Häkkinen et al*. [2011a]. Their (1° resolution) numerical model study shows increases in Gulf Stream transport and subpolar gyre transport during the above time interval (a period of increasing NAO index), with only localized effects of air/sea heat flux variability.

[12] The subpolar OHC PC1 (and the North Atlantic PC2) shows that the heat content evolves from the warm decades of the 1950s–1960s to cold decades of the 1970s, 1980s, and early 1990s and to warming again after the mid-1990s. The subpolar North Atlantic is well known to have lagged behind and even cooled while much of the world ocean warmed [e.g., *Levitus et al.*, 2012; *Willis et al*., 2004]. This evolution matches the recent period of Atlantic multidecadal variability [*Enfield et al*., 2001; *Ting et al*., 2009; HRW]. In HRW, we attributed the AMV to the wind stress curl gyre mode, which is the second leading mode of wind stress curl variability in the North Atlantic sector (the

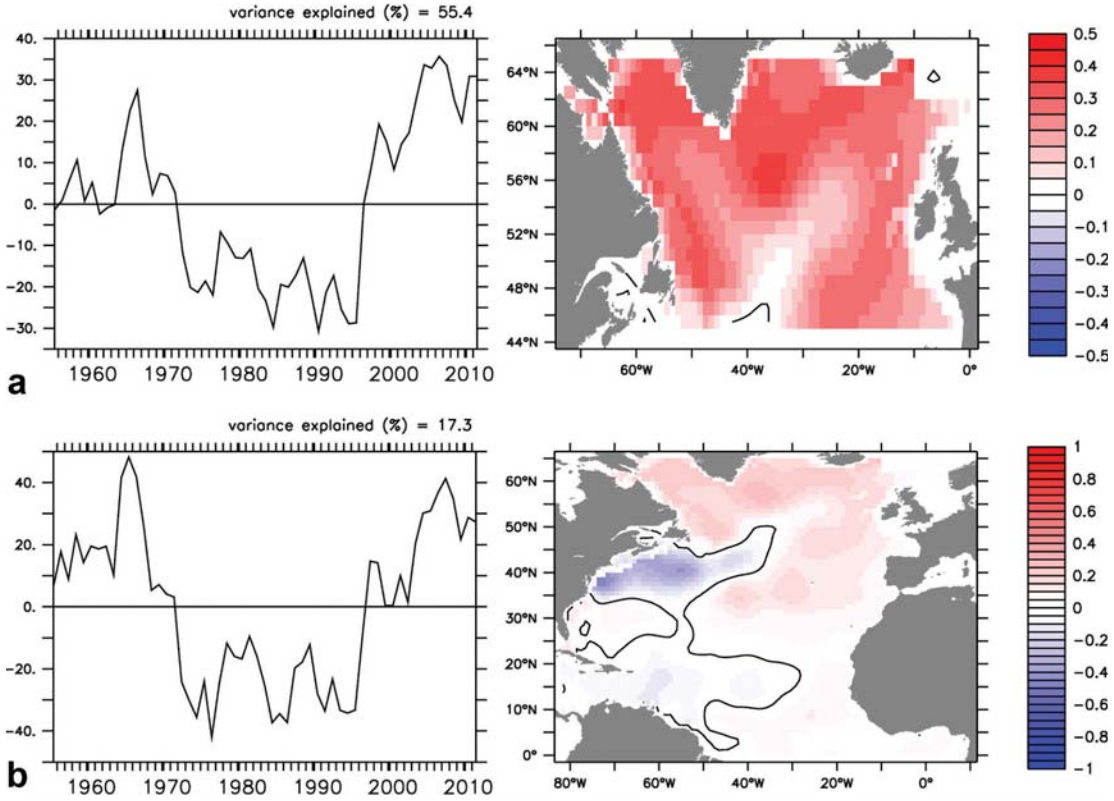

Figure 4. (left) PC1 and (right) EOF1 of the subpolar-only NODC 700 m heat content (limited to 45°N–65°N). Units are 10^{18} J for PC1 and dimensionless for EOF1. (left) PC2 and (right) EOF2 of the whole North Atlantic NODC 700 m heat content for 0°–65°N. Units are 10^{18} J for PC1 and dimensionless for EOF1.

NAO is often invoked in this region, but it is associated with the first EOF mode, with a center of action straddling subpolar/subtropical gyre boundary unlike EOF mode 2); the wind stress curl EOFs and PCs are shown in Figure S2. On the other hand, this gyre mode couples a weakening subpolar (and subtropical) gyre with enhanced access of subtropical waters into the subpolar gyre via the eastern branches of NAC [*Häkkinen et al*., 2011a]. In Figure 5a we show both the wind stress curl PC2 and the subpolar 0 to 700 m OHC PC1 for 1955–2011. The overall impression implies a close and simultaneous relationship between the low-frequency gyre mode of wind forcing (its interannual variability is smoothed out) and heat content variability, weaker gyre corresponding to higher heat content. The relationship suggests that the local Ekman pumping associated with the wind stress curl would be effective in modulating the OHC. The differences in the early period are not surprising given that either NCEP/NCAR Reanalysis or NODC ocean data may not have had optimum data coverage and data quality. Nevertheless, we realize that the time series is too short to establish such correlations rigorously.

[13] Returning to more recent decades where the OHC and the altimetric SSH have an upward trend, the comparison of the SSH PC1 with subpolar area average OHC for the altimeter period is shown in Figure 5b. Both the OHC and SSH PC1 show a cooling-warming sequence in 2009–2010. The abrupt change of SSH PC1 in 2010 does not translate equally intensely in the subpolar OHC. The intensity of SSH PC1 2010 event may originate from lower-latitude processes (discussed in section 5), and also from the fact that due to the more extensive area of the subtropics than of the subpolar gyre, the area weighted EOF analysis gives more weight to subtropical processes than to the subpolar processes. Locally to the subpolar gyre, Figure 5c shows that the linkage between OHC and altimetric SSH is especially tight over the boundary currents of the subpolar gyre. (SSH-OHC covariance has its own variability as discussed earlier.) Overall due to the trends in SSH and OHC (1993–2011), they are highly correlated also in the rest of the North Atlantic, except on the western side over the Gulf Stream and the Guiana Basin. Correlations over 0.6 are significant at 99% level. For period 1993–2003 *Willis et al*. [2004] showed positive correlations for the GS-NAC region. Now using longer time series, this correlation over GS-NAC has reversed its sign and diminished, and the high correlation pattern resembles the spatial patterns of the OHC variability associated with AMV (Figure 4b).

[14] While the subpolar OHC and the weakening gyre, as expressed by SSH PC1, are highly correlated for the altimetry period, it is not obvious why they should be so closely related. Mapping OHC change from 1993–1997 to 2007–2011 along with the mean current field from AVISO (Figure 6a), we see that the OHC changes are concentrated in the boundary currents, especially evident around the Greenland and Labrador seas. Independent support for the warming of near-surface waters in the 1960s and late 1990s is given by *Buch et al*.

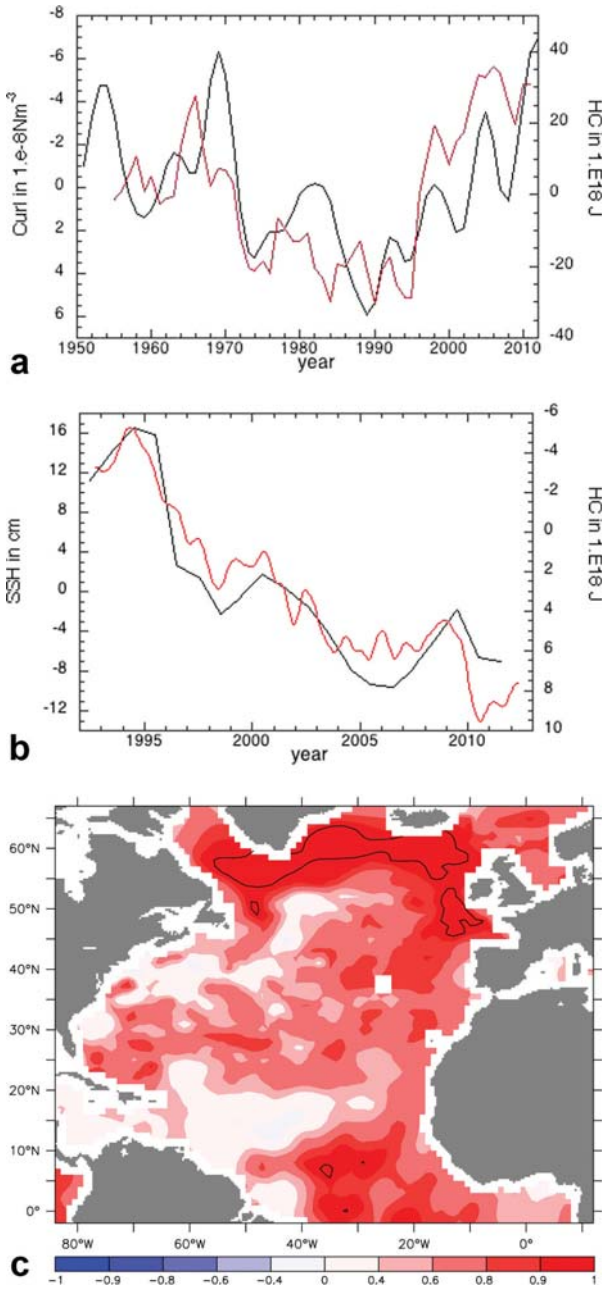

Figure 5. PC2 of wind stress curl (derived NCEP/NCAR data) for EOF mode 2 (black) and PC1 of ocean heat content (NODC 0–700 m; red). SSH PC1 (red) and average heat content in the subpolar gyre (annual data, the last data point at 2011; black; axis inverted). Correlation between NODC OHC (0–700 m) and annual altimetric SSH from MEaSUREs project for period 1993–2011. The area contoured by a black line marks correlation values above 0.95. Values above 0.6 are significant at 99% level.

[2004] from annual hydrographic surveys on the west Greenland continental shelf (on Fylla Bank).

[15] In the eastern subpolar gyre the Rockall Trough shows the advection of warmer subtropical waters as already suggested by changes in surface drifter paths and deep hydrographic changes [*Häkkinen and Rhines*, 2009; *Häkkinen et al*., 2011a]. *Sherwin et al*. [2012] describe the long historical record of Rockall Trough water masses, including variability of nutrient fields and estimate that about one half of the warm subtropical waters destined to reach the Nordic Seas flow through Rockall Trough. (We note here that the reprocessed surface drifter data set [*Lumpkin et al*., 2013] continues to show penetration of subtropical drifters, though sparse, to the subpolar gyre after year 2000 originating from the warm side of GS (Figure S3).) Particularly, the southern branch of NAC at about 45°N, east of 30°W, is associated with a significant warming signal. The highest heat content changes in the eastern region, between 40°N and 50°N, are located where we found increased eddy kinetic energy starting around year 2000, suggestive of shifts in strength/activity of the NAC branches [*Häkkinen and Rhines*, 2009, Figures 8 and 9b]. Mapping the heat content change with the geostrophic current changes for the whole North Atlantic (from MEaSUREs project to emphasize larger scales) between the early and the late pentad (Figure 6b) shows that positive heat content anomalies are associated with anticyclonic current anomalies and negative ones with cyclonic current anomalies. This relation applies both in the subpolar gyre and in the subtropics. Hence, the heat content anomalies have a baroclinic, dynamic origin, such as shifts/changes in currents.

[16] The shift of the eastern NAC branches between the mid-1990s and late 2000s is visible in the section along 48°N (from NOAA/NODC pentadal hydrography) east of 30°W (Figure 6c), which passes through the pattern of strong OHC variability (Figure 6a). The subtropical water "bowl" has expanded eastward where the maximum temperature changes occur in the top 600 m. The negative heat content anomaly is also visible in this section from changes of the main NAC branch between 40°W and 30°W. The increased OHC anomaly in the eastern Atlantic is fed be the southern branch of NAC. Importance of changes in the NAC in the subpolar warming is also apparent from the 20°W repeat section by *Johnson and Gruber* [2007] which shows that the high apparent oxygen utilization signal of Mediterranean Water origins reaches Rockall region at or below $\sim 27.5\sigma_0$ ($\sigma_1 = 32.0$). This isopycnal is at 1000 m depth at 30°N and rises to 750 m depth at 50°N–55°N; hence, the lighter, warmer waters above are likely arriving from the NAC route.

[17] Salinity variability accompanies these OHC changes, and the evolution of the Θ/S diagram over time (not shown) verifies that temperature anomalies dominate the water density variability; thus, the strong subpolar warming since mid-1990s is also a reduction in mean upper ocean density and is not associated with "heaving" of isopycnals. As waters move from the Gulf Stream/NAC region northeastward they mix with more saline eastern Atlantic waters: thus, the Lagrangian circulation origins of subpolar waters lie both in the Gulf Stream and the eastern Atlantic.

5. Abrupt Change of 2010: Atmospheric Blocking

[18] SSH PC1 has an abrupt change in 2010. As we show earlier, SSH PC1 is an analog to the wind stress gyre mode, which governs both of the North Atlantic gyres. The 2010 change is indicative of the gyre weakening also in the subtropical gyre. The wind stress gyre mode is a result of storm tracks moving southward due to atmospheric blocking

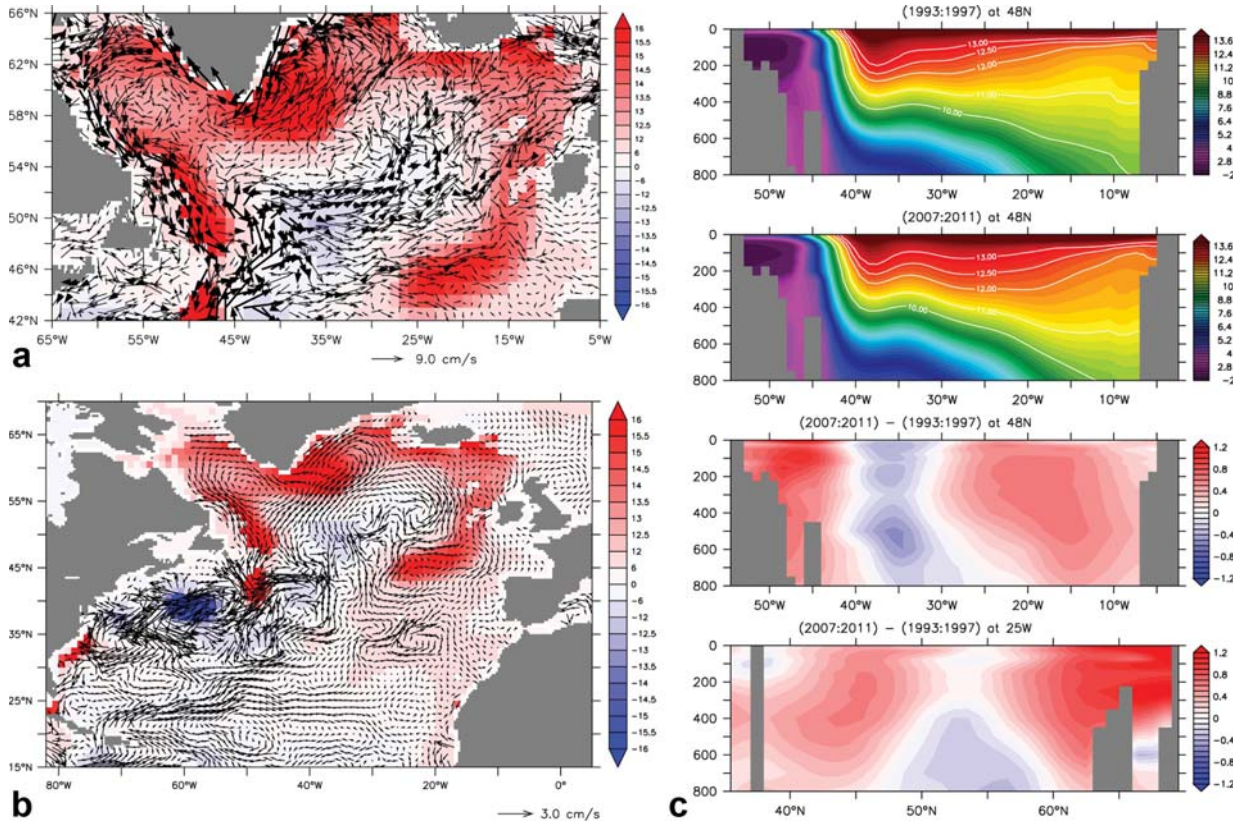

Figure 6. NODC 700 m OHC change from 1993–1997 to 2007–2011 mapped against the time-mean surface currents from AVISO. Magnitude of the thick vectors is twice the scaling of the thin vectors. NODC 700 m OHC change from 1993–1997 to 2007–2011 mapped against the surface current anomalies from MEaSUREs project. NODC pentadal temperature data (top) 1993–1997 and (middle) 2007–2011 at 48°N. Isotherms of 13°C, 12.5°C, 12°C, 11°C, and 10°C are plotted to highlight the spatial changes. Temperature differences at 48°N and 25°W are shown in the bottom figures. Salinity variability is positively correlated with this temperature variability, yet with much less effect on density.

(HRW). Associated with such movement, the westerlies move southward where the largest impact should be visible in the Ekman transport. In the RAPID (Research with Adaptive Particle Imaging Detectors) meridional overturning circulation (MOC) time series (http://www.noc. soton.ac.uk/rapidmoc/home.html) [*McCarthy et al*., 2012] during December 2009 and early 2010 the Ekman transport reversed; during that time the MOC also briefly reversed. Other large Ekman transport reversals occurred in winters 2004/2005 and 2010/2011 [*McCarthy et al*., 2012]. Winter 2009/2010 was highly active in blocking (75 days within December-March period; 61 days of Greenland blocking) as were winters 2010/2011 (94 blocking days; 52 days of Greenland blocking) and 2004/2005 (94 blocking days; 66 days of Greenland blocking). To demonstrate southward movement of the westerlies we plot zonal averages of the zonal wind stress for December-March in 2009, 2010, 2011, and 2012 (Figure 7a). The zonal wind stress reversed in a wide band between 25°N and 30°N in December 2009, and 2010, January 2010, and February 2010. During these reversals also the subpolar wind patterns became highly anomalous; the westerlies weakened or the subpolar winds became easterlies. Hence, the zonal wind stress was highly anomalous at all latitudes, maximum westerlies around 35°N which would normally be located in the subpolar gyre. For these reversals to occur, blocking over the Greenland side, i.e., negative NAO phase (seen also in Table 1), is more important in forcing the jet stream to its furthest southern location (and zero curl line parallels latitude about 35°N) [*Woollings et al*., 2008]. The wind stress curl anomaly in winter 2009/2010 (for Dec-Jan-Feb (DJF)) is shown in Figure 7b which is the typical anomaly associated with the negative NAO index.

6. Discussion

[19] The recent, extensive warming of the subpolar Atlantic and Nordic Seas is associated with changing surface currents and also shifting balance of source waters for the NAC. Here we establish deep-reaching connections between the surface and EOF structure of water column heat content, the warming extending to at least 800 m depth (Figures 4a, 4b, and 6) [*Häkkinen and Rhines*, 2009].

[20] As first noted in the analysis of Simple Ocean Data Assimilation (SODA) data [*Häkkinen et al*., 2011a], we can now fully appreciate the role of the wind stress curl gyre mode in the modulation of the subsurface subpolar heat and salt content. It is responsible for the heat content variability over the five recent decades based on the observational data

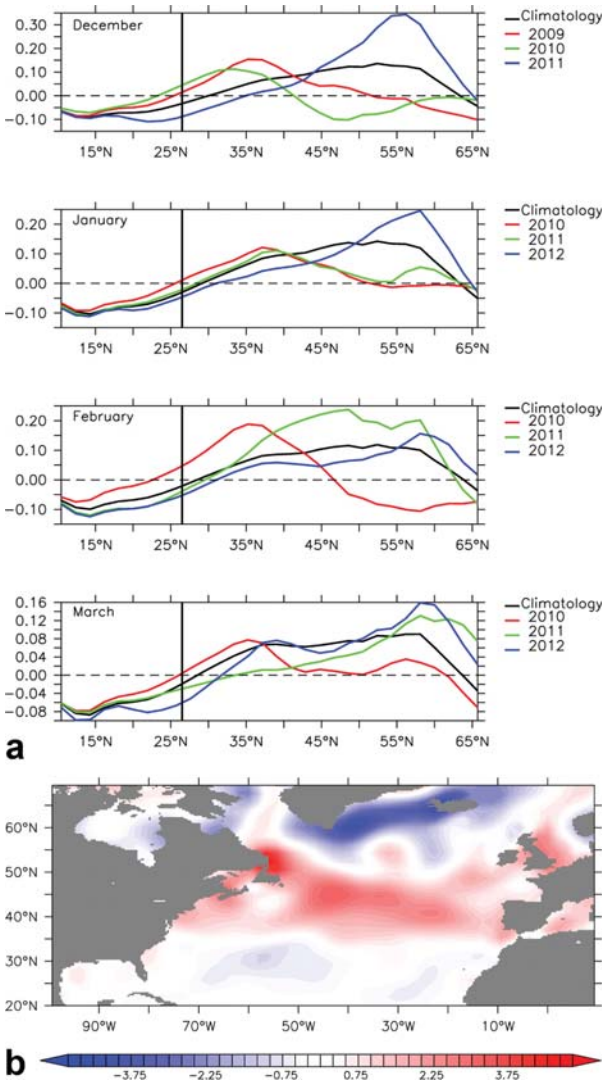

Figure 7. (a) Zonal average of monthly zonal wind stress (in N/m^2) for December-March for winters 2009–2012 and the corresponding monthly climatology. The black vertical lines denotes latitude 26.5°N, location of RAPID array. (b) The wind stress curl anomaly for winter 2009/2010 (DJF) from the DJF mean for 1951–2010 from NCEP/NCAR reanalysis. Unit is 10^{-7} N/m^3.

as shown here, and this control covers much of the observational record to the early twentieth century as indicated by several data sources: the gyre mode and atmospheric blocking activity covary with the Atlantic multidecadal SST variability (HRW). These augment the more commonly used NAO pattern (∼EOF1 of wind stress curl) by allowing for east-west movement of atmospheric forcing patterns and stronger correlation with the mean gyre positions. The (zonally averaged) vertical temperature variability 1920–1997 in the North Atlantic displays a mode with time series similar to AMO/AMV and shows deep warming in the subpolar gyre and central subtropics when AMO/AMV is in a warm phase [*Polyakov et al*., 2010].

[21] Investigation of the most recent period using the altimetric SSH data shows the increase of the subpolar gyre sea surface height continuing almost linearly from 1994 to 2012 (Figure 2). SSH consists both dynamic effect and steric effect from heating and cooling. The observed top 700 m ocean heat content over the altimeter period shows a close relation to the time series of the first SSH EOF mode and extends the time series back to the 1950s; *Reverdin*'s [2010] work and our AMV discussion (HRW) continue the record of warm episodes back to the early 1900s.

[22] However, directly focusing on the high-resolution altimetric geostrophic velocities, we find that the signal is concentrated in the subpolar boundary currents and is particularly visible in the western subpolar gyre. In the south-central subpolar gyre the hydrography shows expansion and deepening of subtropical waters in the NAC, thereby supplying excess heat to the subpolar boundary currents. This emphasizes the impact of advection of heat from lower latitudes on SSH competing with the influence of local heat exchange. Using data from 1955 to 2011 for wind stress curl and heat content, the heat content variability can be attributed to the wind stress gyre mode which modulates transport of subtropical waters into the subpolar gyre with additional impact from the associated heat exchange which amplifies the advected anomalies (HRW). Based on the gyre mode evolution for the last two decades, the almost monotonic subpolar SSH increase in the altimetric record is consistent with the AMV variability.

[23] The subsurface circulation is complex, with regional differences from the surface deceleration in the subpolar gyre, as shown in the core of the Irminger Gyre by *Vage et al*. [2011]. Pathways for warm, high-salinity water to transit from subtropics to subpolar gyre are not completely understood. We have emphasized the western route through the North Atlantic Current, but even there, on its northward path between 40°N and 52°N the NAC loses much of its transport to a broad eastward, eddy-rich drift. This and the occurrence of eddy intensity variability throughout the transition zone between subtropics and subpolar latitudes make it likely that the mixing between western and eastern Atlantic sources of warm water is variable in time and contributing to the history of warm episodes reaching high latitude. Pathway variability has been identified in numerical model simulations; deep eastern pathways involving Mediterranean Overflow Water are described by *Burkholder and Lozier* [2011], and *Desbruyeres et al*. [2013] use a ∼15 km resolution model to describe shifting Lagrangian pathways, out of phase with the amplitude of the AMOC. Their variability from the 1960s to 2000s suggests three episodes of expansion of the subtropical gyre into the subpolar latitudes even as the volume transports of both components of the NAC decline (the two components of NAC correspond with its subtropical and subpolar origins, respectively). Their model largely reproduces the observed decadal variability of 3-D warm subtropical penetration northward, as established from observations by *Häkkinen et al*. [2011a]. Of these three episodes, the late 1990s–2000s warm invasion of the high subarctic stands out, blending with the century timescale AMV.

[24] The only unusual event in the altimetric SSH PC1 time series is an abrupt change in 2010 superimposed on the almost monotonic decrease. This change is simultaneous with a significant drop of several Sv in the MOC, with a temporary reversal of MOC, in the RAPID MOC time series [*McCarthy et al*., 2012]. We attribute these changes to the atmospheric

blocking/negative NAO in the Greenland sector, forcing the storms to pass further south than normal, hence leading to mean winds to be westerly instead of easterly. Thus, the blocking activity has an immediate influence on the subtropical Ekman transport, and indeed the RAPID time series shows that the 2010 drop comes mostly from the Ekman transport which reversed its sign during winter 2009/2010.

[25] Whether the SSH PC1 trend itself is a sign of MOC behavior or not, some prognostic modeling studies are converging to show a general MOC decline during the altimeter period [e.g., *Desbruyeres et al*., 2013; *Fan and Schneider*, 2012; *Deshayes and Frankignoul*, 2008; *Häkkinen et al*., 2008]. Further studies are needed to show whether and how we can use altimetric SSH (combined with ARGO floats) to quantify Atlantic MOC on decadal and longer time scales. A promising study using a high-resolution hybrid coordinate ocean model (HYCOM) simulation of *Xu et al*. [2013] shows that AMOC at 53°N, the Labrador Sea SSH and OHC, the subpolar gyre intensity, and the deep western boundary current volume are all correlated.

[26] **Acknowledgments.** S.H. and D.L.W. gratefully acknowledge the support from NASA Headquarters Physical Oceanography Program and OSTM Science Team for this work. P.B.R. is supported by NASA through the OSTM Science Team. Altimeter data were provided by Brian Beckely, supported by NASA's MEaSUREs program. Also, we thank the two anonymous reviewers for constructive and helpful comments.

References

Bersch, M., I. Yashayaev, and K. P. Koltermann (2007), Recent changes of the thermohaline circulation in the subpolar North Atlantic, *Ocean Dyn.*, *57*, 223–235, doi:10.1007/s10236-007-0104-7.

Buch, E., S. A. Pedersen, and M. H. Ribergaard (2004), Ecosystem variability in West Greenland waters, *J. Northwest Altlantic Fish. Sci.*, *34*, 13–28.

Burkholder, K. C., and M. S. Lozier (2011), Mid-depth Lagrangian pathways in the North Atlantic and their impact on the salinity of the eastern subpolar gyre, *Deep Sea Res.*, *Part I*, *58*, 1196–1204, doi:10.1016/j.dsr.2011.08.007.

Daniault, N., H. Mercier, and P. Lherminier (2011), The 1992–2009 transport variability of the East Greenland–Irminger Current at 60°N, *Geophys. Res. Lett.*, *38*, L07601, doi:10.1029/2011GL046863.

Desbruyeres, D., V. Thierry, and H. Mercier (2013), Decadal variability of meridional overturning circulation, *J. Geophys. Res.*, doi:10.1029/2012JC008342, in press.

Deshayes, J., and C. Frankignoul (2008), Simulated variability of the circulation in the North Atlantic from 1953 to 2003, *J. Clim.*, *21*, 4919–4933, doi:10.1175/2008JCLI1882.1.

Enfield, D. B., A. M. Mestas-Nunez, and P. J. Trimble (2001), The Atlantic multidecadal oscillation and its relation to rainfall and river flows in the continental U.S., *Geophys. Res. Lett.*, *28*(10), 2077–2080, doi:10.1029/2000GL012745.

Fan, M., and E. K. Schneider (2012), Observed decadal North Atlantic tripole SST variability. Part I: Weather noise forcing and coupled response, *J. Atmos. Sci.*, *69*, 35–50.

Häkkinen, S., and P. B. Rhines (2004), Decline of subpolar North Atlantic gyre circulation during the 1990s, *Science*, *304*, 555–559.

Häkkinen, S., and P. B. Rhines (2009), Shifting surface currents of the northern North Atlantic Ocean, *J. Geophys. Res.*, *114*, C04005, doi:10.1029/2008JC004883.

Häkkinen, S., H. Hatun, and P. B. Rhines (2008), Satellite evidence of changes in the Northern Gyre, in *The Role of the Northern Seas in Climate*, edited by R. R. Dickson, J. Meincke, and P. Rhines, pp. 551–568, Springer, Dordrecht, the Netherlands.

Häkkinen, S., P. B. Rhines and D. L. Worthen (2011a), Warm and saline events embedded in the meridional circulation of the northern North Atlantic, *J. Geophys. Res.*, *116*, C03006, doi:10.1029/2010JC006275.

Häkkinen, S., P. B. Rhines, and D. L. Worthen (2011b), Atmospheric blocking and Atlantic multi-decadal ocean variability, *Science*, *334*, 655–659, doi:10.1126/science.1205683.

Hátún, H., B. Hansen, A. B. Sandø, H. Drange, and H. Valdimarsson (2005), De-stabilization of the North Atlantic Thermohaline Circulation by a gyre mode, *Science*, *309*, 1841–1844.

Johnson, G. C., and N. Gruber (2007), Decadal water mass variations along 20W in the Northeastern Atlantic Ocean, *Prog. Oceanogr.*, *73*, 277–295.

Joyce, T. M., and R. Zhang (2010), On the path of the Gulf Stream and the Atlantic meridional overturning circulation, *J. Clim.*, *23*, 3146–3154.

Knight, J. R., R. J. Allan, C. K. Folland, M. Vellinga, and M. E. Mann (2005), A signature of persistent natural thermohaline circulation cycles in observed climate, *Geophys. Res. Lett.*, *32*, L20708, doi:10.1029/2005GL024233.

Knight, J. R., C. K. Folland, and A. A. Scaife (2006), Climate impacts of the Atlantic multidecadal oscillation, *Geophys. Res. Lett.*, *33*, L17706, doi:10.1029/2006GL026242.

Knutsen, Ø., H. Svendsen, S. Østerhus, T. Rossby, and B. Hansen (2005), Direct measurements of the mean flow and eddy kinetic energy structure of the upper ocean circulation in the NE Atlantic, *Geophys. Res. Lett.*, *32*, L14604, doi:10.1029/2005GL023615.

Levitus, S., et al. (2012), World ocean heat content and thermosteric sea level change (0–2000 m), 1955–2010, *Geophys. Res. Lett.*, *39*, L10603, doi:10.1029/2012GL051106.

Lumpkin, R., S. A. Grodsky, L. Centurioni, M.-H. Rio, J. A. Carton, and D. Lee (2013), Removing spurious low-frequency variability in drifter velocities, *J. Atmos. Oceanic Technol.*, *30*, 353–360.

Mahajan, S., R. Zhang, T. L. Delworth, S. Zhang, A. J. Rosati, and Y.-S. Chang (2011), Predicting Atlantic meridional overturning circulation (AMOC) variations using subsurface and surface fingerprints, *Deep Sea Res., Part II*, *58*, 1895–1903.

McCabe, G. J., M. A. Palecki, and J. L. Betancourt (2004), Pacific and Atlantic Ocean influences on multidecadal drought frequency in the United States, *Proc. Natl. Acad. Sci. U. S. A.*, *101*, 4136–4141, doi:10.1073/pnas.0306738101.

McCarthy, G., E. Frejka-Williams, W. E. Johns, M. O. Baringer, C. S. Meinen, H. L. Bryden, D. Rayner, A. Duchez, C. Roberts, and S. A. Cunningham (2012), Observed interannual variability of the Atlantic meridional overturning circulation at 26.5°N, *Geophys. Res. Lett.*, *39*, L19609, doi:10.1029/2012GL052933.

Polyakov, I. V., V. A. Alexeev, U. S. Bhatt, E. I. Polyakova, and X. Zhang (2010), North Atlantic warming: Patterns of long-term trend and multidecadal variability, *Clim. Dyn.*, *34*, 439–457.

Reverdin, G. (2010), North Atlantic Subpolar Gyre surface variability (1895–2009), *J. Clim.*, *23*, 4571–4584, doi:10.1175/2010JCLI3493.1.

Sarafanov, A., A. Falina, A. Sokov, and A. Demidov (2008), Intense warming and salinification of intermediate waters of southern origin in the eastern subpolar North Atlantic in the 1990s to mid-2000s, *J. Geophys. Res.*, *113*, C12022, doi:10.1029/2008JC004975.

Scherrer, S. C., M. Croci-Maspoli, C. Schwierz, and C. Appenzeller (2006), Two-dimensional indices of atmospheric blocking and their statistical relationship with winter climate patterns in the Euro-Atlantic region, *Int. J. Climatol.*, *26*, 233–249.

Sherwin, T. J., J. F. Read, N. P. Holliday, and C. Johnson (2012), The impact of changes in the North Atlantic gyre distribution on water mass characteristics in Rockall Trough, *ICES J. Mar. Sci.*, *69*, 751–757.

Ting, M., Y. Kushnir, R. Seager, and C. Li (2009), Forced and internal twentieth-century SST trends in the North Atlantic, *J. Clim.*, *22*, 1469–1481.

Vage, K., R. S. Pickart, A. Sarafanov, Ø. Knutsen, H. Mercier, P. Lherminier, H. M. vanAken, J. Meincke, D. Quadfasel, and S. Bacon (2011), The Irminger Gyre: Circulation, convection, and interannual variability, *Deep Sea Res., Part I*, *58*, 590–614, doi:10.1016/j.dsr.2011.03.001.

Willis, J., D. Roemmich, and B.Cornuelle (2004), Interannual variability in ocean heat content, temperature and thermosteric expansion at global scales, *J. Geophys. Res.*, *109*, C12036, doi:10.1029/2003JC002260.

Woollings, T., B. J. Hoskins, M. Blackburn, and P. Berrisford (2008) A new Rossby-wave breaking interpretation of the North Atlantic Oscillation, *J. Atmos. Sci.*, *65*, 609–626.

Xu, X., H. E. Hurlburt, W. J. Schmitz Jr., R. Zantopp, J. Fischer, and P. J. Hogan (2013), On the currents and transports connected with the Atlantic meridional overturning circulation in the subpolar North Atlantic, *J. Geophys. Res.*, doi:10.1002/jgrc.20065, in press.

Zhai, X., and L. Sheldon (2012), On the North Atlantic Ocean heat content change between 1955–70 and 1980–95, *J. Clim.*, *25*, 3619–3628.

Zhang, R. (2008), Coherent surface-subsurface fingerprint of the Atlantic meridional overturning circulation, *Geophys. Res. Lett.*, *35*, L20705, doi:10.1029/2008GL035463.